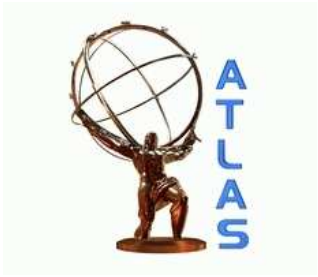

ATLAS NOTE

ATL-COM-TILECAL-2008-018

February 6, 2009

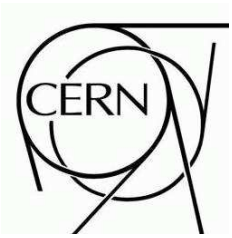

Time Calibration of the ATLAS Hadronic Tile Calorimeter using the Laser System

Christophe Clément[1], Björn Nordkvist[1], Oleg Solovyanov[2], Iacopo Vivarelli[3]

[1] *Stockholm University, Sweden,*
[2] *Institute for High Energy Physics (IHEP), Russia*
[2] *INFN, Sezione di Pisa, Italy*

ATL-TILECAL-PUB-2009-003
09 March 2009

Abstract

The ATLAS Tile Calorimeter (TileCal) will be used to measure i) the energy of hadronic showers and ii) the Time of Flight (ToF) of particles passing through it. To allow for optimal reconstruction of the energy deposited in the calorimeter with optimal filtering, the phase between the signal sampling clock and the maximum of the incoming pulses needs to be minimised and the residual difference needs to be measured for later use for both energy and time of flight measurements. In this note we present the timing equalisation of all TileCal read out channels using the TileCal laser calibration system and a measurement of the time differences between the 4 TileCal TTC partitions. The residual phases after timing equalisation have been measured. Several characteristics of the laser calibration system relevant for timing have also been studied and a solution is proposed to take into account the time difference between the high and low gain paths. Finally we discuss the sources of uncertainties on the timing of the Tile Calorimeter.

1 Introduction

The ATLAS Tile Calorimeter (TileCal) will be used to measure i) the energy of hadronic showers and ii) the Time of Flight (ToF) of particles passing through it. To allow optimal reconstruction of the energy deposited in the calorimeter with optimal filtering [1], the phase between the signal sampling clock (at 40 MHz) and the incoming pulses needs to be known to better than 1 ns. We refer to the phase between the pulse maximum and the sampling clock as the *"T_{fit}"*, whose calculation will be further detailed later.

Prior to beam, available data consists of i) calibration runs, ii) cosmic muon runs. In both cases the phase between the sampling clock and the pulse (calibration or cosmic muon induced) is not fixed from event to event. Nevertheless the difference between T_{fit} in any channel with T_{fit} in a selected reference channel does not change from event to event. TileCal has nearly 10,000 read-out channels, so there are about 10,000 such delays. By measuring these offsets with respect to the selected reference channel and programming corresponding delays in the front end electronics of TileCal, the 10,000 degrees of freedom are reduced to a single phase with respect to the 40 MHz sampling clock which can finally be adjusted the day the sampling clock is synchronised with the beam.

In this paper we describe the determination of these channel-to-channel delays using the TileCal laser calibration system and present the resulting timing uniformity. The remaining sources of uncertainties are underlined and a comparison with first beam data [2] is presented.

2 The ATLAS Tile Calorimeter

2.1 TileCal

The ATLAS hadronic Tile Calorimeter [3] [4], also called TileCal, is a scintillating sampling calorimeter [5] named after its layers of scintillating plastic tiles and steel absorbers plates. Its main task is to identify jets and perform measurements of their energy and direction, as well as to contribute to the measurement of missing transverse energy. TileCal is also capable of measuring the ToF of particles crossing it [6]. TileCal also plays an important role in the ATLAS Level-1 (LVL1) trigger [7], hence a fast read out system is required.

TileCal has a cylindrical structure (Fig. 1) divided into a 5.64 m "long-barrel" (LB) and two 2.65 m "extended-barrels" (EB), with an inner radius of 2.28 m and an outer radius of 4.23 m and with a total coverage of $|\eta| < 1.7$. The long barrel itself is divided into two partitions, or an A- and an C-side, called LBA and LBC respectively. Each of the extended barrels makes up its own partition, EBA and EBC respectively. Each partition is sub-divided into 64 azimuthally oriented wedge shaped modules shown on Fig. 2), making a total of 256 TileCal modules.

Secondary charged particles produced in hadronic showers will cross the scintillators which emit light. The light is collected by wavelength-shifting fibers (WLS) and distributed to PMT's. The PMT's together with supply electronics and readout electronics are placed in a girder at the back of each module. Each barrel module contains 45 PMT's and an extended barrel module contains 32 PMT's.

The tiles are arranged in cells as shown in Fig. 3. The WLS fibers from all tiles within one cell are organized in two bundles, one from each side of the cell. The bundles are in turn connected to two different PMT's placed in the girder. Also as shown in Fig. 3 the tiles are grouped into readout cells organized into 3 different radial depths: A-cells closest to the beam line (z-direction), D-cells furthest away from the beam line and so called BC-cells in the intermediate region. The three sampling depths are staggered in z in order to obtain a geometry pointing towards the interaction point.

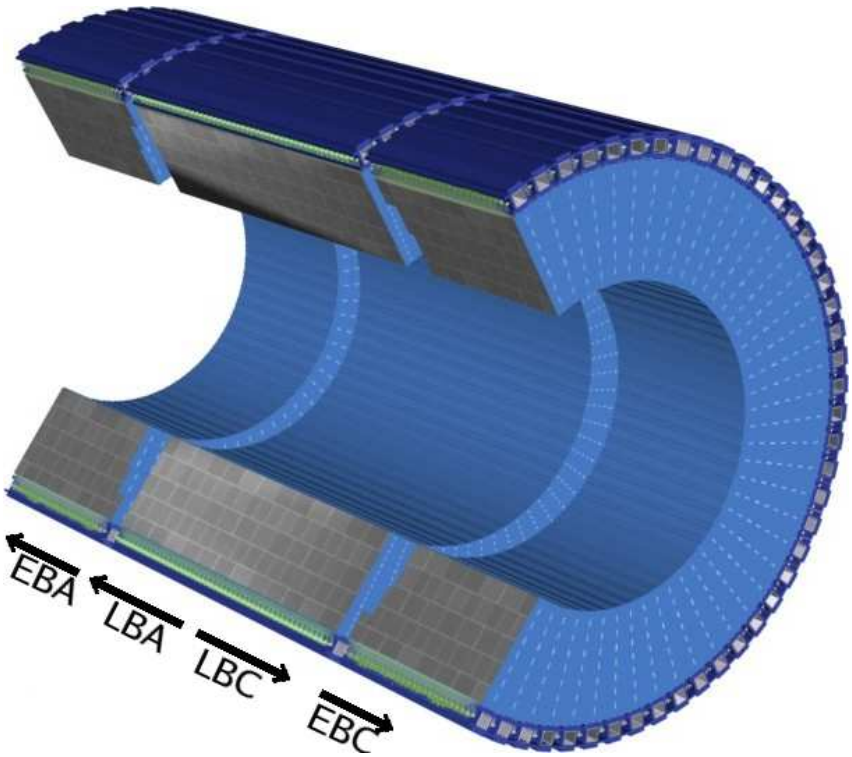

Figure 1: The ATLAS Tile Calorimeter and its four partitions.

2.2 TileCal Electronics and Readout

The photomultipliers together with the front-end electronics [8] are mounted on so-called drawers (Fig. 4) which are movable and can be inserted into the girder, located at the back of each module (Fig. 2). The analogue signals from the PMT's are shaped and amplified by a so-called 3-in-1 card attached to the PMT base. The 3-in-1 card has four signal outputs: one for the first level trigger, one for calibration purpose and two outputs to the digitizer board. The last two have different amplification, labelled as high (HG) and low gain (LG), with a ratio of 64 in order to be sensitive to a wide range of signal strength.

2.2.1 The Digitizer Board

The purpose of the TileCal digitizer system [9] is to sample and digitize the analogue signals coming from the PMT's via the 3-in-1 cards. The digitizer board has two 12-bit Analogue to Digital Converters (ADCs), two for each PMT, reading the HG and LG outputs respectively. The ADCs sample the analogue signals from the 3-in-1 card every 25 ns. The sampled values are buffered in a local pipeline memory while awaiting the first level trigger accept (L1A). The digitizer board also contains one Timing Trigger and Control receiver chip (TTCrx) described in Section 2.2.3, and two TileDMUs, described in section 2.2.4. One digitizer reads out and digitizes the analogue signals from up to six PMT's. One barrel drawer has eight digitizers (and 45 PMT's) while an extended barrel drawers has only six digitizers (and 32 PMT's). The PMT to digitizer mapping is given in Tables 2 and 3.

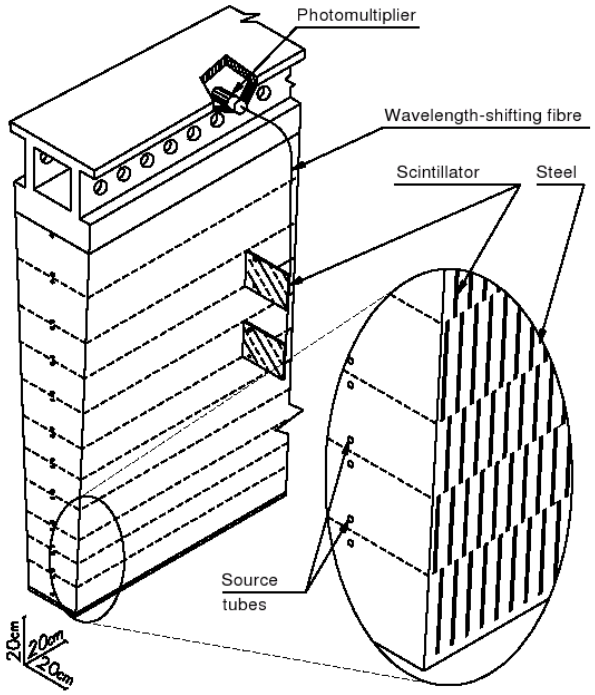

Figure 2: A wedge shaped TileCal module. A module has 11 tile rows, consisting of alternating layers of scintillating plastic and steel absorbers. The tiles are oriented perpendicular to the beam line. The holes in the side distribute the Cs^{137} source tubes used for calibration. On top of the module lies the "drawer", containing the PMT's and the front-end electronics.

2.2.2 ATLAS Timing, Trigger and Control

The ATLAS Timing, Trigger and Control (TTC) system [10] is a multipurpose, optical fiber based, distribution system that has been developed for the four LHC experiments. The TTC system distributes timing, trigger and control information, trigger accepts, bunch crossing counters, orbit signals, trigger type, counter resets, and configuration and test commands. The trigger accepts are generated by the ATLAS Central Trigger Processor (CTP) when TileCal is operated within an ATLAS run, or otherwise from a Local Trigger Processor. The TTC system also distributes the 40 MHz system clock that is synchronized with the protons bunches during LHC collisions.

2.2.3 TTC Receiver Chip

The TTC receiver chip [11] (TTCrx) is an interface between the TTC optical system and the front-end electronics. It receives the optical signals and converts them into electrical signals. The TTCrx receives the central 40 MHz clock and distributes a synchronous but delayed clock refered to as `clock40des2`, to the ADCs. The `clock40des2` clock can be delayed which allows for the adjusment of the phase between the physical pulse due to passing particles and the sampling clock. A fine programmable delay, refered to as `dskew2`, allows one to delay the `clock40des2` clock by up to 25 ns, in steps of 0.104 ns. In this work, the `dskew2` delays are used to compensate for different arrival times of the 40 MHz system clock to different parts of TileCal front-end electronics.

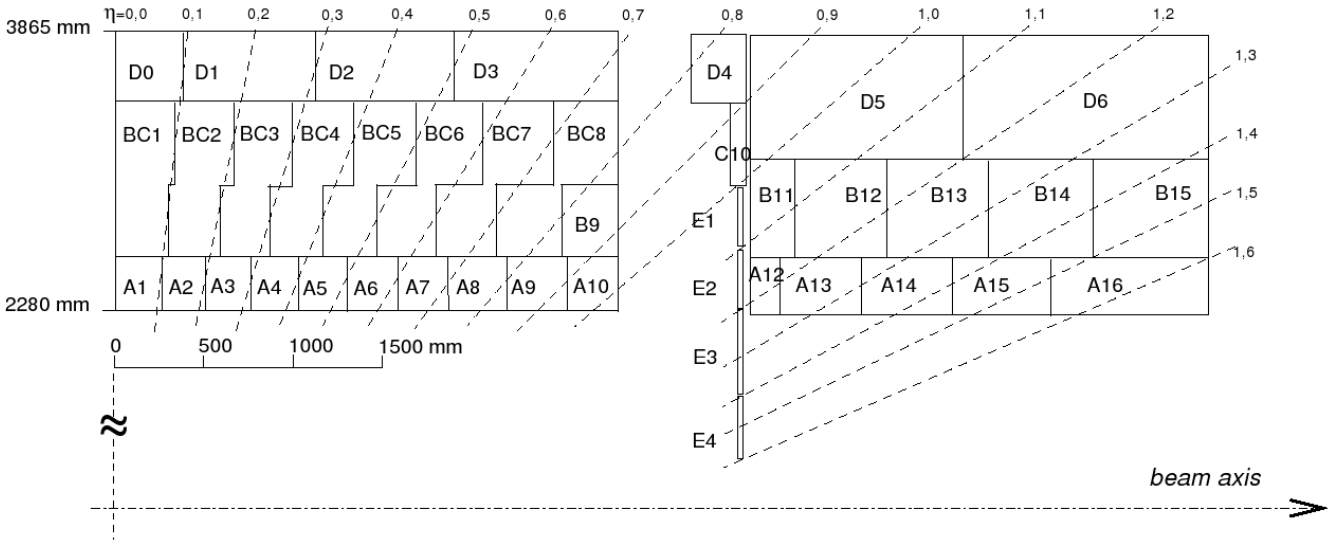

Figure 3: Sketch of the Tile Calorimeter showing cell structure and cell numbers. The left side of the figure shows a barrel module (such as LBA or LBC) and the right side shows an extended barrel module (such as EBA or EBC). The three readout depths: A-, BC- and D-cells as well as lines of constant η are displayed.

2.2.4 TileDMU

The TileDMU [12, 13] (Data Management Unit) chip, located on the digitizer board, is a readout- and digitizer-control system. It contains the pipeline memory which stores the sampled data for up to 6.4 μs, while waiting for the LVL1 trigger accept. When the LVL1 trigger decides to keep an event, a level-1 accept (L1A) signal is sent to the TileDMU from the ATLAS CTP via the optical TTC system and the TTCrx. The TileDMU then, for the selected gain, reads out 7 consecutive samples from the pipeline memory. The pipeline memory can be set such that the readout starts one or several samples later or earlier. This provides a handle for coarse timing in multiples of 25 ns. This setting can be seen effectively as a programmable delay which is refered to as Δp in the rest of this work.

2.3 TileCal Timing

It has been found [11] that the best time and energy estimate is obtained when the ADCs samples are within 2.0 ns from the top of the analogue pulse. This means that when using seven samples to record an event, the fourth sample should be within 2.0 ns of the pulse peak. The quantity measuring the time difference between the fourth sample and the pulse maximum is called "the calculated time" or T_{fit} (illustrated in Fig. 6a) and is calculated by the TileCal reconstruction, with the so-called "fit method" [14]. T_{fit} is defined as

$$T_{fit} \equiv t_{peak} - t_{4^{th}}, \tag{1}$$

where $t_{4^{th}}$ is the absolute time of the 4^{th} sample on the pulse. The sign of T_{fit} can be interpreted in terms of late or early sampling of the pulse, in the following way:

$$T_{fit} \begin{cases} > 0 & \Rightarrow \text{The sampling of the pulse by the ADC starts too early} \\ < 0 & \Rightarrow \text{The sampling of the pulse by the ADC starts too late} \end{cases}$$

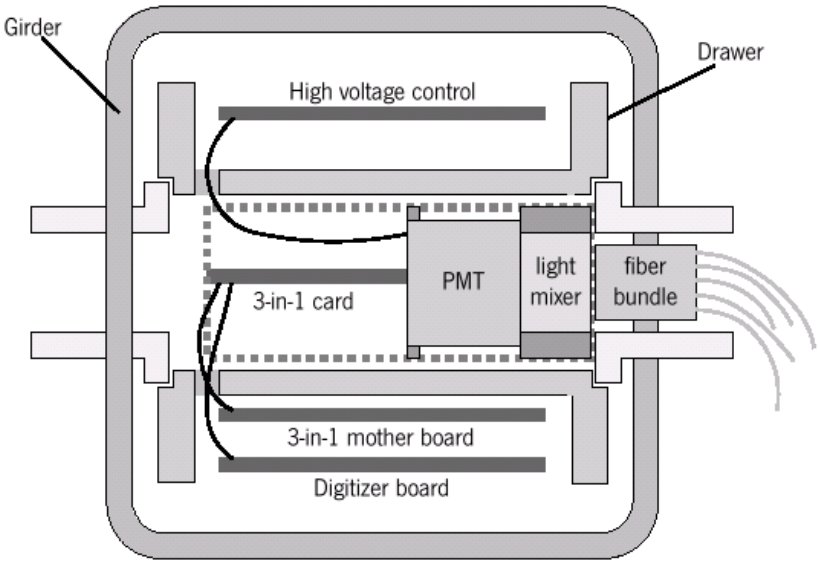

Figure 4: Cross-section of a drawer, showing the fiber bundle (WLS fibers) coming from the scintillating tiles, the PMT and its associated electronics.

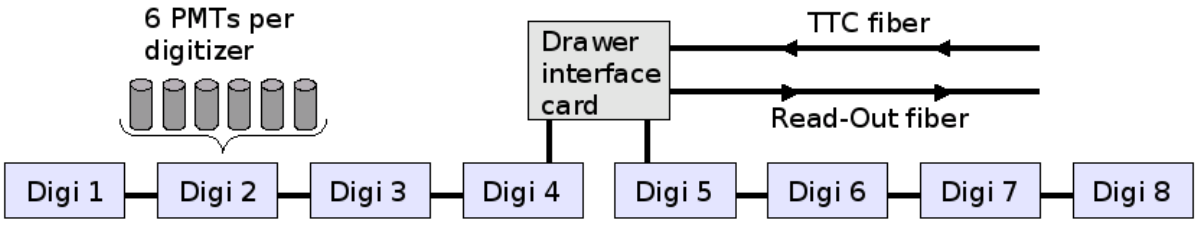

Figure 5: Propagation of the TTC signals inside a TileCal barrel drawer, from the interface card to the digitizer boards. The TTC fiber comes from the counting room located about 100 m away from the ATLAS cavern.

In the ideal situation $T_{fit} = 0$ for all channels. However there are a number of reasons why this is not the case *a priori*:

- The 40 MHz system clock is provided to each digitizer board by the TTC system (as shown in Fig. 5) via the TTCrx. The signal enters each drawer via an interface card placed at the center of each barrel drawer or at one side of each extended barrel drawer. Thereafter the signal propagates through adjacent boards on its way through the drawer, delaying the arrival of the system clock up to about 10 ns to the outermost digitizers. A late arrival of the system clock means that the ADC will also sample the pulse late, if not corrected for.

- The TTC fibers running from the counting room to each drawer can have significantly different lengths, due to the large size of TileCal. In the most extreme cases the difference in fiber length is more than 7 m , corresponding to a time difference of up to about 40 ns (as discussed later in Section 4.2). A long TTC fiber means late arrival of the system clock compared to a drawer with a short fiber. Hence the ADCs will sample late if this effect is not corrected for.

- The time of flight for particles to different regions of the calorimeter differs as well as the length of the light collecting WLS fibers. This has to be corrected for before real physics data is taken. However this issue is not addressed in this paper, since the WLS fibers are completely separated from the laser light distribution path.

- Further on, a time difference between high- and low-gain signals of the order of about 2 ns has been observed in test beam [15]. A study in the final calorimeter setup presented in section 5 confirms this result.

The TileDMU is clocked by the 40 MHz system clock, while the ADCs are clocked by the `clock40des2` clock. Both clocks are obtained from the TTCrx. The system clock is fixed (and synchronized with the LHC bunch crossings). The `dskew2` is synchronous with the system clock but delayed by a constant phase. This allows for fine tuning of the ADCs in order to sample as near the PMT pulse peak as possible and to obtain a uniform T_{fit}.

The `clock40des2` clock can be delayed by up to 25 ns, with respect to the system clock. The delay is set in units of `dskew2` counts, where 1 count = 0.104 ns (240 counts represents 25 ns). Six consecutive channels share the same digitizer and the same TTCrx, therefore the TTCrx cannot compensate for delays among the six channels it is connected to. It is also impossible to use the `dskew2` delay to correct for differences between the high gain and low gain paths.

2.4 Signal Reconstruction

The pulse phase and amplitude are reconstructed with the linearized method. The fit method uses prior knowledge of the pulse shape in order to reconstruct the pulse and suppress the noise. For each channel a fit to the function

$$f(t) = Ag(t-\tau)+c \tag{2}$$

is performed, where A is the amplitude, g is the normalized pulse shape function, τ parameterises the peak position in time and c is the pedestal value. The pulse shape function has to be derived separately for physics and calibration data, and is stored for later retrieval by the reconstruction algorithm.

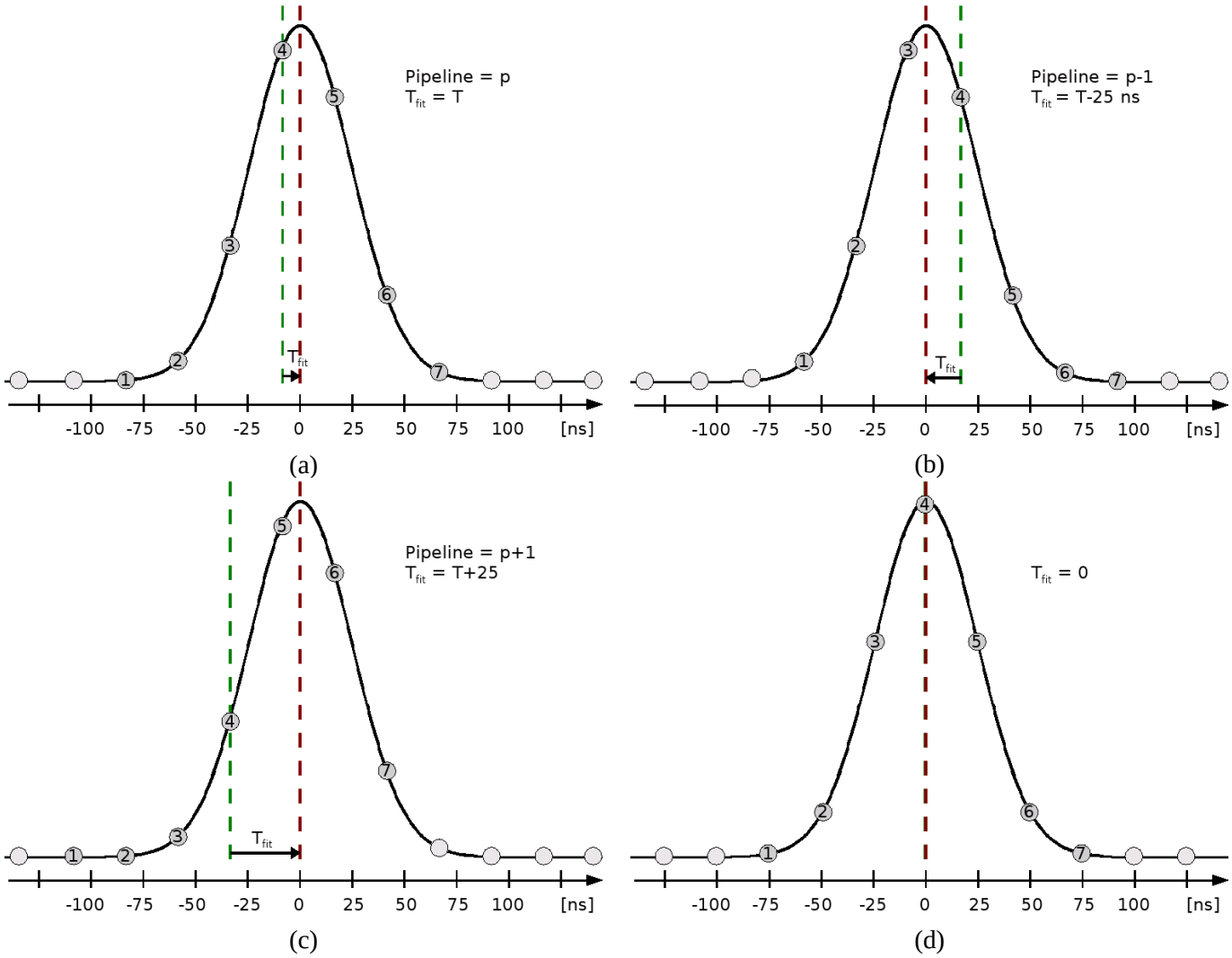

Figure 6: The figure shows the effect of changing the digitizer pipeline memory offset Δp and the `dskew2`, on the calculated time T_{fit}, between the pulse peak and the 4^{th} sample. The numbered circles indicate the seven consecutive samples taken by the ADC and read out. (a) The pulse is sampled too early by the ADC, hence $T_{fit} > 0$. (b and c) The pipeline memory setting Δp is changed by -1 (b) and +1 (c) respectively. This has the effect of changing the 1^{st} sample to be read out (circle numbered 1). (b) The position of the samples can be finely adjusted to achieve $T_{fit} = 0$ by setting `dskew2` to an appropriate value.

3 The Laser System

In order to calibrate and monitor the response of the TileCal PMT's an integrated laser system [16] has been developed. Laser pulses with a wavelength of 532 nm and a pulse width of 15 ns from a single laser source are distributed directly into each of TileCal 9852 PMT's via a chain of optical fibers. In the present work, the laser system is used for the time calibration of TileCal.

3.1 Laser Distribution System

A sketch of the laser system is displayed in Fig. 7. The laser is located in an underground counting room (USA15) about 100 m away from the ATLAS calorimeter. The light is collected from the laser box and sent into a beam expander box, via a single liquid fiber. The beam expander box then splits the laser light into 384 fibers, each of them being connected to an adjustable connector on to a patch panel at the back of the laser rack. To the same connectors on the patch panel, are then connected 384 so-called laser fibers, each about 110 m (120 m) long in the barrel (extended barrel).

The laser fibers lead the laser light to each of the Tile Calorimeter modules. The connectors at the patch panel allow to adjust the size of an air gap between the fibers coming from the beam splitter and the laser fibers, thus allowing to adjust the light intensity sent into each laser fiber. All components upstream the patch panel lead to the same delays for all fibers, due to equal lengths.

The 384 laser fibers distribute the light to all TileCal PMT's as follows. In the extended barrel, there are two laser fibers per module. The laser fibers are connected to "1-17 connectors", there are two such connectors per extended barrel drawer. One distributes the laser light to the even PMTs and the other one to the odd PMTs. In total 256 laser fibers are needed to distribute the light to the two TileCal extended barrels.

Inside the barrel calorimeter, each laser fiber is connected to a "1-50 connector" from which the laser light is split into odd (even) PMT's in an A (C)-side drawers and even (odd) PMT's in the corresponding C (A)-side drawer. Thus 128 laser fibers are needed to distribute the light to all PMT's in the TileCal barrel calorimeter. The WLS fibers, connecting the tiles to the PMT's, are not part of the laser path.

3.2 Light Intensity

The light signal provided by the laser is very similar to that created by particles traversing the detector. Several attenuation filters provide the possibility to monitor the response over the full dynamic range. In the context of this paper the laser system is used to set the correct timing for all channels. For the studies in this paper the constraints on the light amplitude of the laser are of two types:

- Maximize the amount of light sent to the drawers, since the time resolution becomes better for higher pulse amplitudes,
- Make sure that none of the PMT's saturates, otherwise the pulse shapes are distorted and the timing measurement is no longer reliable.

Following these guidelines, the recommended laser settings are: 20,000-23,000 for the laser system intensity setting and filter 6 for low gain, and the same intensity setting but filter 8 for high gain timing. For the special gain study of Sect. 5 the laser was set to an intensity setting of 23000, with the laser filter 2.

3.3 Laser Fiber Lengths

The laser fibers have approximately the same lengths within each partition ($\sim$110 m for LBA/LBC and $\sim$120 m for EBA/EBC). There is a strong indication that the precision of the cutting of the laser fibers

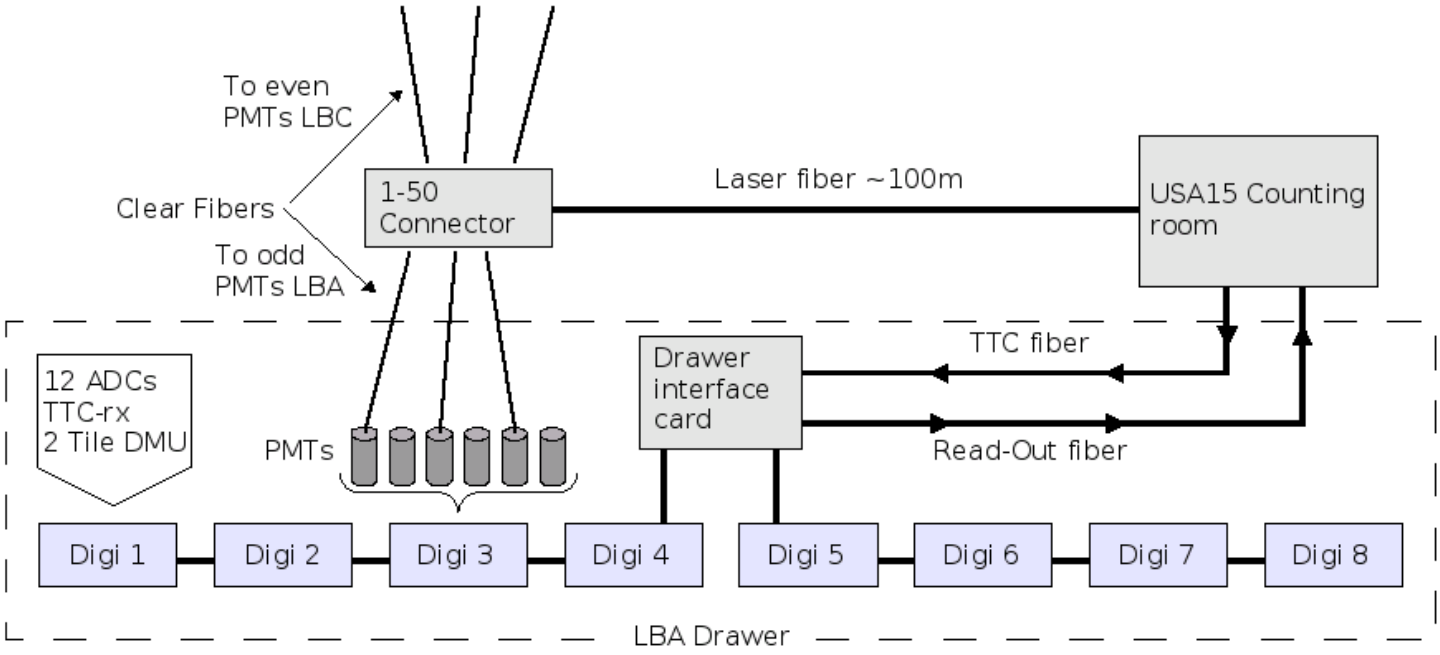

Figure 7: The laser distribution system. The figure shows the laser distribution chain for a TileCal barrel drawer. Note that it takes two laser fibers to distribute light to odd and even PMT's in one drawer.

leads to a smearing of the laser pulse arrival time, with a standard deviation of the order of more than 1 ns. Figure 8 shows the mean time in even PMT's minus the mean time in odd PMT's computed for each barrel drawer. Since the even and odd PMT's are fed with two different laser fibers, whose length should be the same, the spread of this distribution gives an estimate of the accuracy of the laser fiber cutting. From this plot we conclude that it is of the order of 1.2 ns in the barrel. This method cannot be applied to the extended barrel, since for extended barrel drawers all PMT's of a given drawer are fed by the same laser fiber.

A systematic measurement of the laser fiber lengths was carried out [17]. These measurements provide the laser fiber lengths with an average precision of 1-2 ns, which is not precise enough to resolve the laser fiber length differences within the same TileCal partition. Nevertheless these measurements are useful to derive the relative timing of the different TileCal partitions, as discussed in Section 4.3.

The clear fibers are of different lengths (see Tables 2, 3 in appendix A and B). These lengths are taken into account in the intra-module time equalization described in Sec. 4.1.

3.4 Speed of Light in the Clear and Laser Fibers

In order to exploit the laser calibration data to derive delays between channels and partitions, it is necessary to know the velocity of light, in the optical fibers that make up the TileCal laser distribution systems, for the wavelength used by the laser system. The laser and clear fibers are of the same type and thus have the same velocity of light, which we denote v_{CF}. There are several available measurements of v_{CF}. From the manufacturer [18] it is specified that v_{CF}=20.1 cm/ns. There is also a "direct measurement" of v_{CF} performed using an OTDR [17], but at a wavelength of 648.8 nm instead of 532 nm for the operating wavelength of the laser system and gives v_{CF}=20.4$\pm$0.1 cm/ns. The variation of v_{CF} between these two wavelengths should nevertheless be of the order of a few percents.

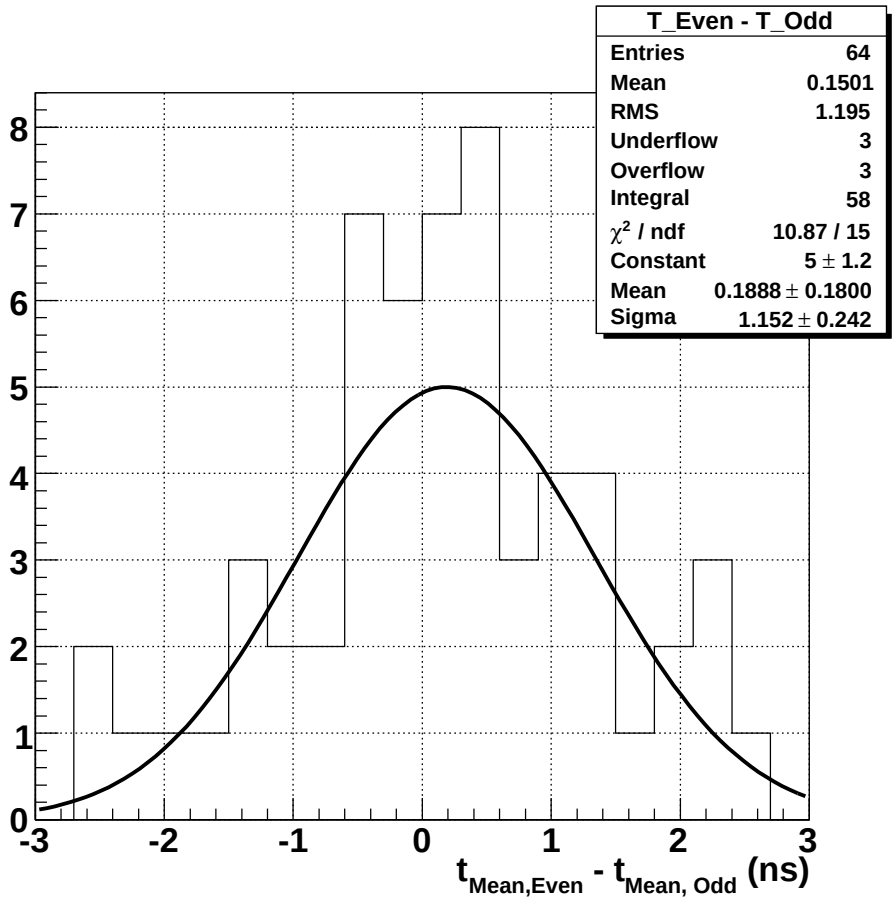

Figure 8: Distribution of the time difference between even and odd PMTs in the 64 barrel super-drawers.

In the rest of the present paper we used the value calculated by the ”iterative method”, presented below, namely, v_{CF}=22.5 cm/ns. It is this value that was used to derive the delays that were actually used in TileCal during the first LHC beam in 2008.

The measurements of v_{CF} presented below are all consistent with the velocity given by the manufacturer as well as the direct OTDR measurement presented in Ref. [17]. Nevertheless the precision of these measurements is somewhat low, with uncertainties in the range 1.2 to 2 ns. Without new and more precise measurements of v_{CF} in situ, the value of v_{CF} provided by the manufacturer, seems to be the most reasonable to use for any future recalculation of the TileCal delays.

3.4.1 Iterative method

We performed a measurement of v_{CF} by measuring T_{fit}, as function of the clear fiber lengths. The difference in clear fiber lengths between two contiguous PMT's is known to be 11.6 cm. Since the length differences are known, the measured difference between T_{fit} values can be used to extract v_{CF}. Nevertheless a second contribution to the T_{fit} differences arises from the propagation of the TTC clock itself. This contribution is not apriori known. In order to unfold the two contributions, we use an iterative method. We first assume a certain value of v_{CF}, which allows us to compute the contribution due to the

delays of the clock. Using these TTC delays, the velocity v_{CF} can be fitted. The fitted value of v_{CF} can then be reused to rederive the delays due to the clock propagation. This can be repeated until the fitted value of v_{CF} does not change anymore.

The first step of the iterative procedure uses the initial value of v_{CF} =18 cm/ns, as measured in test-beam [15]. The value of v_{CF} stabilizes after 2 iterations. At the first iteration we obtain v_{CF} =22.5±2cm/ns. The second iteration yields v_{CF} = 22.3±2 cm/ns.

Note that due to a given uncertainty on the exact routing of the clear fibers in the second half of the TileCal drawers, we use only the first half drawers for this measurement. This question is discussed further in section 6. Even PMT's share a same series of clear fibers with lengths increasing in steps of 11.6 cm. Odd PMT's share a second series of clear fibers with same incremental lengths between PMT's 1, 3, 5, ... Therefore the velocity v_{CF} is derived separately for even and odd series of PMT's, giving two measurements of v_{CF} per drawer. The distribution of measured velocities for 128 drawers is shown in Figure 9.

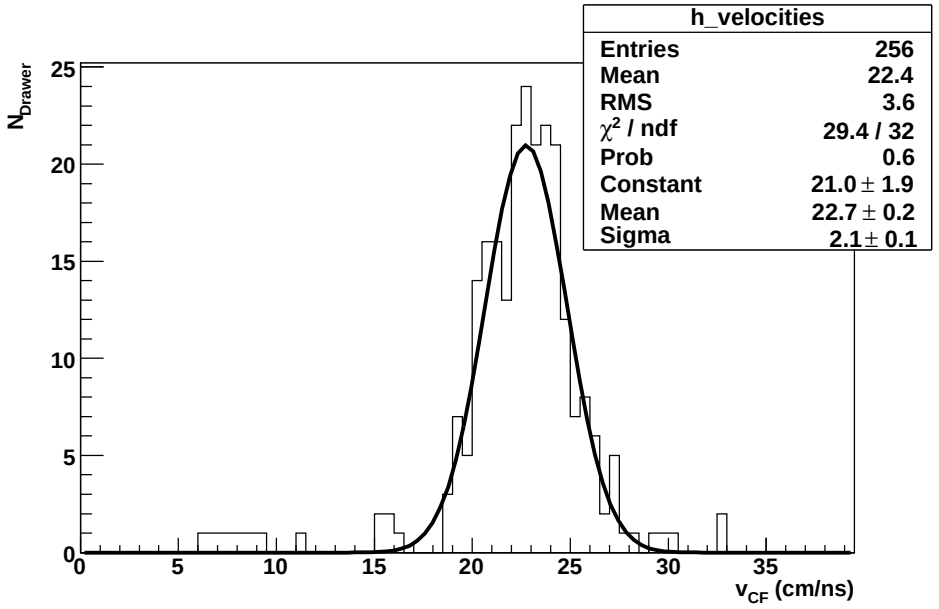

Figure 9: Distribution of the speed of light in laser fibers, v_{CF}, measured with the iterative method, using 128 TileCal barrel drawers. The measurements are carried out only in the 1st half drawer and separately for odd and event PMT numbers, thus giving 2 measurements per drawer.

3.4.2 Per-digitizer method

The iterative method uses the observed variation of T_{fit} over the digitizers in the first half drawer to extract v_{CF} and therefore requires to take into account the clock propagation from digitizer to digitizer. To avoid this problem we consider a second method, refered to as the "per digitizer" method, where we fit v_{CF} only to the T_{fit}'s belonging to the same digitizer. Because the PMT's belong to the same digitizer, there is no delay due to clock propagation. There are six PMT's per digitizer, split into two different series of clear fibers. Therefore we perform two fits of v_{CF} per digitizer, one for the even PMT's and one from the odd PMT's. The main drawback of this method is that each measurement of v_{CF} relies on the fit of a straight line to 3 points, thus leading to an uncertainty on the slope, significantly bigger than the iterative method. Again as for the iterative method, only the first half drawer is considered. Finally the

first PMT of each drawer is used as reference for the time and therefore its time has no error bar. This implies that there are only two points to constrain v_{CF} for the odd PMT's of the first digitizer. These two points are therefore not used, leaving 7 fits per drawer. The resulting distribution of v_{CF} obtained with the "per digitizer method" is shown in Figure 10. The distribution is much wider than for the iterative method. The most probable value is close to 20 cm/ns, but the distribution of fitted velocities is asymmetric and has a large RMS. The asymmetry is due to the fact that the fit is actually performed to $1/v_{CF}$ which is itself Gaussian. This method is not precise enough to extract a usable estimate of v_{CF} with this method.

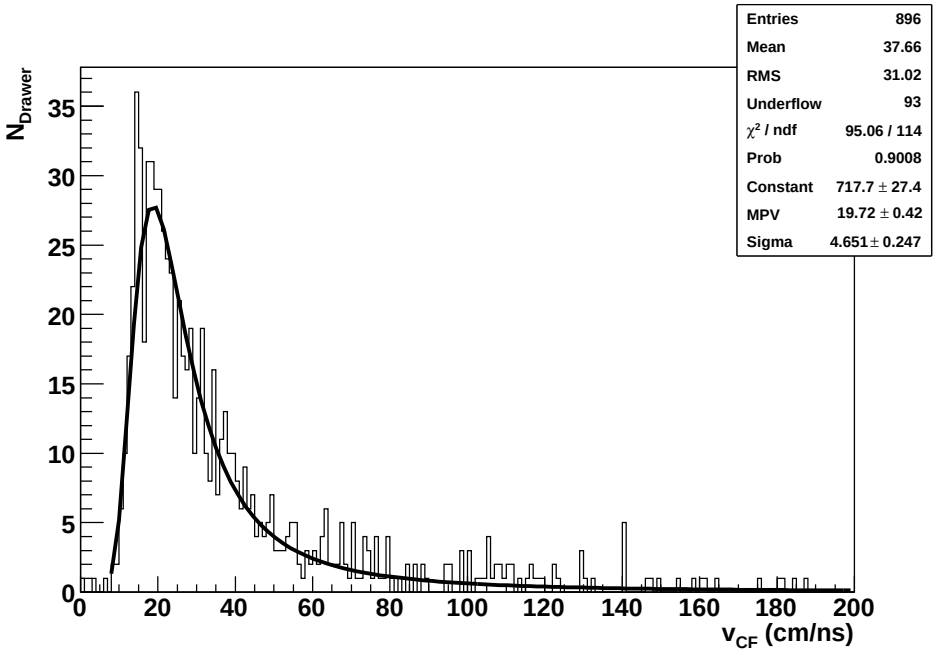

Figure 10: Distribution of the speed of light in laser fibers, v_{CF}, measured with the "per digitizer" method, using 128 TileCal barrel drawers. The measurements are carried out only in the digitizers of the 1st half drawers, separately for odd and even PMT numbers, thus giving 7 measurements per drawer.

3.4.3 Fit to beam data

A third approach fits v_{CF} to the beam data as follows. A global time offset between the barrel and extended barrel partitions can be derived with the laser system, by combining i) the measured difference in T_{fit} between barrel and extended barrel, with ii) the known laser fiber lengths and with iii) the speed of light v_{CF} in the laser fibers. More details concerning the time difference between partitions are given in section 4.3. This estimate of the time difference between barrel and extended barrel is thus a function of v_{CF} which can be fitted to the time difference between barrel and extended barrel *measured* using beam events. We therefore fit v_{CF} to the barrel/extended barrel time difference measured in Ref. [2], which is independent from any of the laser system characteristics. As shown in Fig. 11, the fit yields v_{CF}=21.2$\pm$1.2 cm/ns. The dominating source of uncertainty in this fit is the uncertainty on the laser fiber length. This result is refered to as the "fit to beam" method.

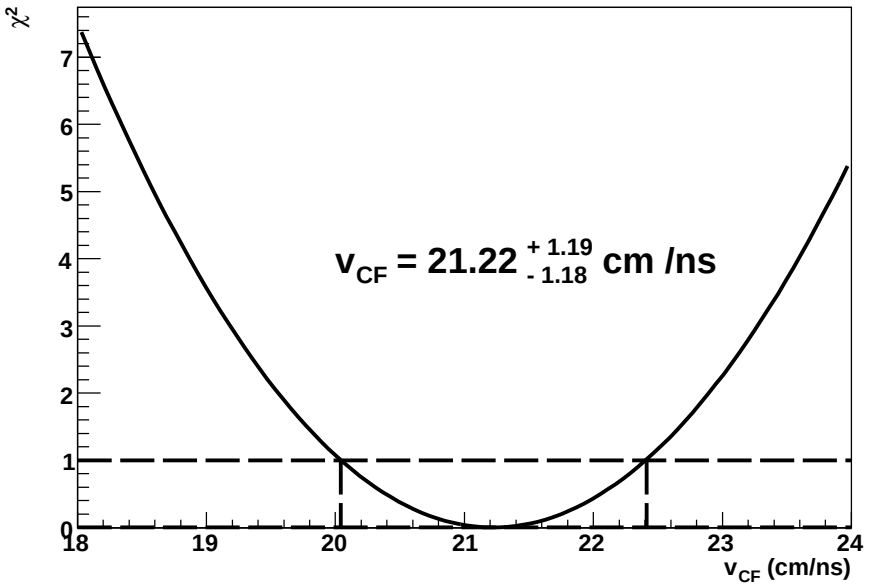

Figure 11: The χ^2 between the partition delays measured in beam events and the predicted partition delays based on the laser data and the speed of light in the laser fibers, as a function of the speed of light in the laser fibers. The best fit gives v_{CF} =21.2$\pm$1.2 cm/ns.

4 Time Calibration of TileCal

A "laser run" corresponds to a set of TileCal data taken while the laser is pulsing. A laser run used for timing analysis normally contains between 3000 and 10000 events or triggers, that is the number of laser pulses sent to each PMT. Each pulse is sampled seven times with at intervals of 25 ns. The pulses are reconstructed using the fit method described in section 2.4. The time between the fourth sample (the sample in the middle) and the reconstructed pulse maximum is known as "the calculated time", or T_{fit} (see section 2.3 and equation 1). For optimal energy reconstruction the sampling of the pulse should occur nearby its maximum, or equivalently T_{fit} should be close to zero. The residual phase between the sampling clock and the pulse maximum, i.e. the residual value of the T_{fit} once the delays in the front electronics have been adjusted, also needs to be known with precision and used as input to the optimal filtering [1].

From the observed T_{fit} values in a laser run, one can derive programmable delays, so-called `dskew2` and digitizer pipeline offsets Δp, so that T_{fit} is made uniform over the entire calorimeter for a simultaneous energy deposition. The following index convention is used: i to refer to PMT's of digitizer j in drawer k of partition l.

4.1 Intra-module Synchronization

Intra-module synchronization refers to the equalization of T_{fit} within each drawer. In the TileCal barrel the signals of the 40 MHz sampling clock propagate from the digitizers in the middle of the drawer towards the digitizers at the end of the drawers, as illustrated in Fig. 5. Thus the sampling clock arrives earlier in the middle of the drawer compared to the extremeties. This leads the PMT's pulses to be sampled earlier in the middle of the drawer compared to the extremeties, as illustrated in Fig. 6. In the extended barrel the clock signals propagate from one end of the drawer to the other end, leading to PMT's pulses sampled earlier at one end of the drawer compared to the other.

The clock signal propagation results in groups of 6 PMT's belonging to the same digitizer to appear as displaced in time with respect to PMT's from the other digitizers. The time difference between two neighbouring digitizers are typically of the order of 2-4 ns (Figure 13a). The goal is to delay the "early" digitizers, the digitizers first receiving the clock signal, in such a way that all digitizers within the drawer sample the PMT's pulses simultaneously. This is done by setting the `dskew2` TTCrx chip delay on the digitizer boards, to an appropriate phase relative to the system clock, hence delaying the time of the samples, as shown in Fig. 13b).

4.1.1 Calculation of Digitizer Corrections

The relative time difference between channels within a drawer are determined from T_{fit}. First the time differences introduced by the laser system itself have to be corrected for. These are:

- Differences in length of the clear fiber, distributing the laser light from the 1-50 connectors to the PMT's.
- Differences in laser fiber lengths causing a time difference between odd and even channels (c.f. routing of laser fibers described in section 3).

The clear fibers have known lengths for each PMT and are listed in tables 2 and 3 in appendix. The time difference T_{diff}, of channel i relative to a reference channel, chosen to be channel 1, is given by

$$T_{diff}(i) = T_{fit}(i) - T_{fit}(1) - (L_{CF}(i) - L_{CF}(1))/v_{CF}\,, \tag{3}$$

where $L_{CF}(i)$ is the length in cm of the clear fiber distributing light to PMT of channel i. Figure 12 shows the distribution of T_{diff} for one channel in LBA. To extract the mean value and the width, a Gauss

function is fitted to the distribution. The width, typically of the order of 0.5 ns, provides information about the square sum of the fit method time resolution in channels 1 and i.

Differences in length of the laser fibers have to be treated in another way since the exact length of each individual fiber is not known to a precision better than 1 ns. The laser fibers are supposed to have the same length within each partition, however, differences originating from the fiber routing and cutting process are observed. By computing the mean value of T_{diff} for odd and even channels separately ($\bar{T}^{even}$ and $\bar{T}^{odd}$), and then adding (subtracting) half the difference of the two to every odd (even) channel one can attempt to compensate for the effect of laser fiber length difference within a drawer. However a systematic effect will still remain for the synchronization between drawers. We define the "laser fiber corrected" time difference T_{diff}^{LFC}, in the following way:

$$T_{diff}^{LFC}(i) = \begin{cases} T_{diff}(i) + \frac{1}{2}\delta & \text{i} = 1,3,5,... \\ \\ T_{diff}(i) - \frac{1}{2}\delta & \text{i} = 2,4,6,... \end{cases} \tag{4}$$

$$\delta = \bar{T}^{even} - \bar{T}^{odd} \tag{5}$$

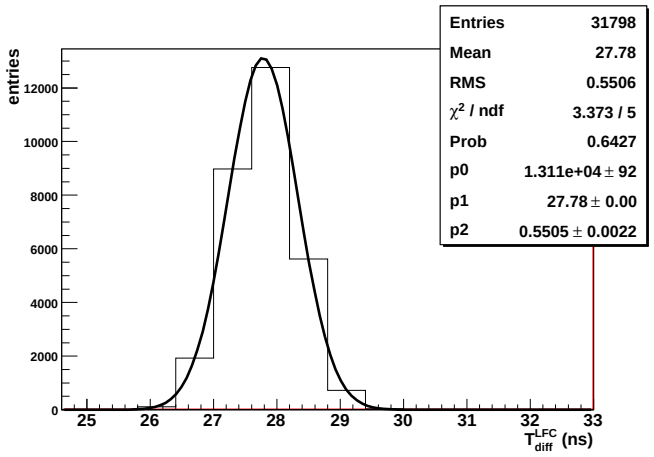

Figure 12: Accumulated T_{diff} in a laser run, from one PMT in LBA. The fit parameters p_0, p_1 and p_2 are the amplitude, mean value and standard deviation respectively.

In order to synchronize the channels in a given drawer, one needs to compute corrections D_{digi}, that can be programmed into each of the drawer digitizers. It is done by computing the mean value of T_{diff}^{LFC} for each digitizer in a drawer, called T_{digi} and take the difference with respect to the first digitizer. We define T_{digi} by:

$$T_{digi}(j) = \frac{1}{N} \sum_{i=m}^{m+N-1} T_{diff}^{LFC}(i) \tag{6}$$

where the sum runs on the N PMT's which belong to digitizer j. The index m is the number of the first PMT of digitizer j. As an example, for the second digitizer in a given drawer, $j = 2$, $m = 7$ and $N = 6$. The correction for digitizer j is given in nanoseconds by:

$$D_{digi}(j) = T_{digi}(j) - T_{digi}(1). \tag{7}$$

The $D_{digi}(j)$ corrections are converted into units of `dskew2` counts (Section 2.3) and rounded to the nearest integer. One `dskew2` count is equal to 104 ps. The maximal value of `dskew2` is 240 which corresponds to a delay of 25 ns. The `dskew2` values are then stored in the TileCal online database used

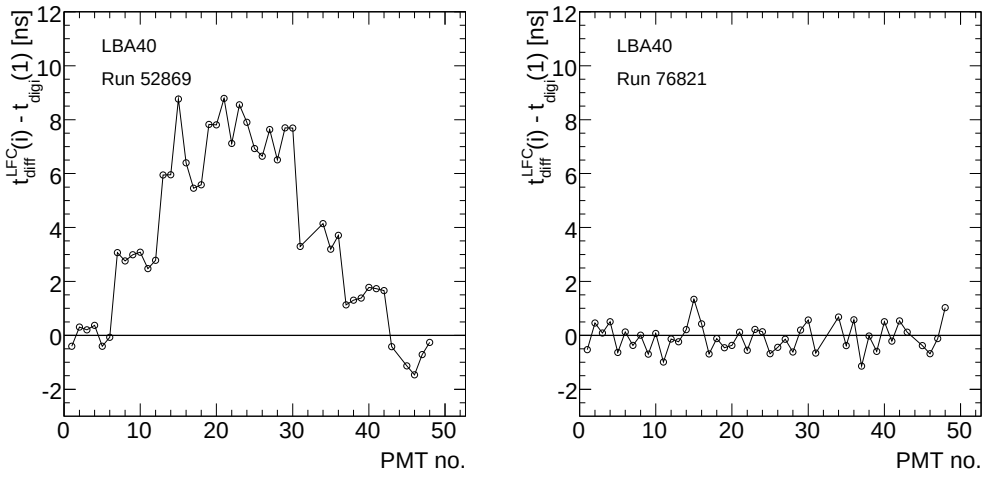

(a) (b)

Figure 13: $T_{diff}^{LFC} - T_{digi}(1)$ vs PMT number, before (a) and after (b) implementing the `dskew2` corrections.

to configure the TileCal front end electronics and data acquisition at the beginning of each TileCal run. It may happen that the computed correction is beyond the allowed `dskew2` range. In this case one has to additionally adjust the TileDMU pipeline offset, Δp. Two situations can occur:

- If the computed `dskew2` correction exceeds 240 counts, the pipeline memory setting of this particular digitizer is changed by Δp=-1 (see Section 2.2.4). This effectively delays the timing of the specific digitizer by one clock cycle, or 25 ns (see section 4.2 and Fig. 6 for details). The computed `dskew2` setting can then be decreased by 240 `dskew2` counts. E.g. if one needs to implement a `dskew2` value of 250, the digitizer pipeline offset is set to Δp=-1 and a `dskew2` of $250 - 240 = 10$ is programmed into the digitizer.

- If, on the other hand, the computed `dskew2` correction is a negative number, the pipeline offset is set to Δp=+1 and the `dskew2` correction is incremented by 240 counts, putting it into its allowed range.

4.2 Inter-module Synchronization

Inter-module synchronization refers to the equalization of T_{fit} among the drawers inside each TileCal partition. Since the TTC fiber lengths differ from drawer to drawer, different drawers receive the clock signals at different times. This changes the phase between the sampling clock and the pulse. During the TTC fiber routing, often the shortest possible fiber length was used. Since TileCal is a large detector this means that the fibers can vary over many meters in length from one drawer to another, generating correspondingly large time differences. Before the start of this work the drawer-to-drawer time difference could be as high as 40 ns.

During the commissioning of TileCal, many of the TTC fibers have been extended in order to obtain a more uniform timing distribution. In the TileCal extended barrel partitions, this would have required a major campaign of TTC fiber adjustment. It was finally decided to use the full functionality of the TileDMU chips on the digitizer boards to implement specific pipeline values for each drawer, in order to compensate for the large differences in TTC fiber lengths. In this way, the T_{fit} can be equalised among drawers, without intervention on the hardware of the TileCal trigger and timing system.

4.2.1 Calculation of Drawer Corrections

The "drawer time" $T_{drawer}(k)$, is defined as the mean value of T_{fit}, corrected for the clear fiber lengths $L_{CF}(i)$, over the first digitizer, i.e. the first six channels (index i) in drawer k:

$$T_{drawer}(k) = \frac{1}{6}\sum_{i=1}^{6}(T_{fit}(i,k) - L_{CF}(i)/v_{CF}). \tag{8}$$

As convention, we choose the drawer 40 of each TileCal partition as reference time, thus $T_{drawer}(k=40)$ defines the "partition reference time" and hence the time reference that all other drawers within the partition are compared to. The time correction of drawer k in units of nanoseconds is thus given by:

$$D_{drawer}(k) = T_{drawer}(k) - T_{drawer}(40). \tag{9}$$

The delays $D_{drawer}(k)$ are then translated in pipeline and fine delay adjustements $\Delta p(k)$ and `dskew2`, given by:

$$\begin{aligned} \Delta p(k) &= int(D_{drawer}(k)/25) \\ \texttt{dskew2} &= 240(D_{drawer}(k)/25 - \Delta p(k)) \end{aligned} \tag{10}$$

The delays computed above are applied to every digitizer in every drawer in order to delay the whole drawer with respect to the reference drawer. In total there are 8 (6) pipeline offsets Δp and 8 (6) `dskew2` values for each (extended) barrel drawer, resulting in approximately 4000 constants stored in the TileCal online database. The constants are produced offline and stored in a file, which is then uploaded manually to the online database, using a script that reads the file with the constants and updates the online database accordingly. The historic of the constants and the software used to produce them is maintained under a dedicated directory in the ATLAS CVS repository [19].

4.2.2 Timing Uniformity after Intra- and Inter-module Synchronisation

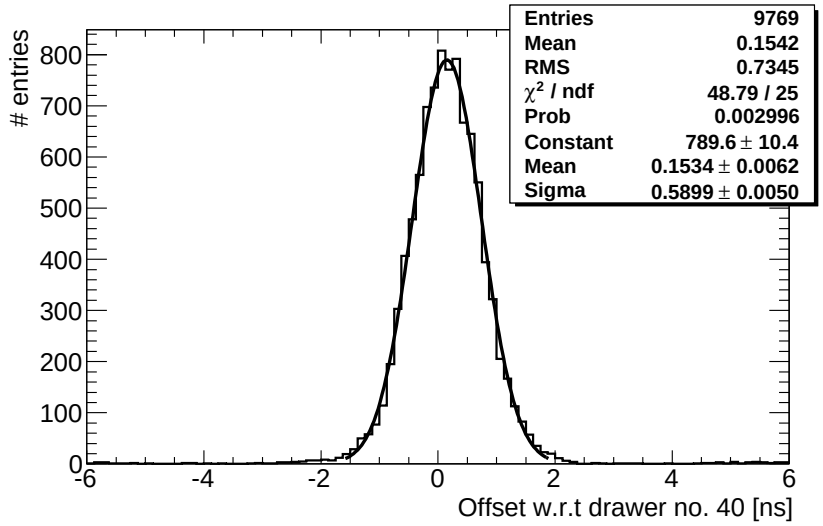

Figure 14: Distribution of T_{fit} after intra- and inter-module synchronisation, with respect to each partition's reference drawer.

Figure 14 shows the resulting distribution of T_{fit}, with respect to the partition reference time, observed for 99% of the TileCal PMT's, in a laser run after intra- and inter- module synchronisation. The given time is measured with respect to the reference drawer of each PMT's respective TTC partition. For this reason the overall time differences between the 4 TileCal partitions are not visible on this histogram but are discussed in details in the next section. We measure a standard deviation of 0.6 ns. Since the timing constants were derived with the laser system and then their performance is evaluated with the laser system again, a number of systematic errors do not appear in this plot. The spread of 0.6 ns is due to the time resolution of the fit method, the limited statistics of the laser run and channel to channel delays within a digitizer. The latter cannot be removed by the use of the programmable delays `dskew2` of the TTCrx chips since there is one TTCrx chip for 6 TileCal read out channels. Additional systematic errors such as the non-uniformity of laser fiber lengths, are not accounted for in this 0.6 ns but are discussed in details in section 6. Fewer than 1% of the TileCal channels are excluded from Fig. 14, because these channels do not yet have proper timing constants, in general due a hardware problem, or an error in the addressing of the front end electronics. Most of the missing channels should be recovered during the 2008-2009 ATLAS winter shutdown.

4.3 Inter-partition Synchronisation

The delays between the different partitions arise from i) different TTC fiber lengths to the 4 partitions, yielding different phases between the physics pulses and the sampling clock, ii) different read out pipelines, iii) different cable lengths between the ATLAS Central Trigger Processor and the various TileCal TTC crates, and possibly iv) different cable lengths among TTC modules inside the TTC crates. Since in earlier sections we showed that the timing can be equalised within each TileCal partition, what remains to be equalised is the peak pulse to sampling clock phase among the reference drawers of the four partitions, which is equivalent to equalising the T_{fit} values among the reference drawers, namely EBA40, LBA40, LBC40 and EBC40 [1)]. The calculation of delays between the reference drawers and their compensation is refered to as the inter-partition synchronisation.

The delays between the reference drawers can be derived using the laser events. We use special runs where the laser system is firing during so-called calibration triggers inside a physics or combined ATLAS run. In this way we measure the inter-partition delays, with the exact same setup as during an ATLAS physics run. This is particularly important as in TileCal standalone and other type of runs, the trigger latencies are not necessarily the same as for an ATLAS combined / physics run, which can therefore require different TileCal pipeline settings.

The difference in drawer time between LBC40 [1)] and the other reference drawers:

$$\begin{aligned} D_{partition}(l) &= T_{k=drawer}(40,l) - T_{drawer}(k=40,LBC) \\ with\ l &= EBA,\ LBA,\ EBC \end{aligned} \tag{11}$$

contains information about the inter-partition delay, but is biased by large differences in laser fiber lengths between partitions. The laser fiber lengths measured in Ref. [17] are used to correct for this effect, thus giving the actual inter-partition delay $P(l)$:

$$\begin{aligned} P(l) &= D_{partition}(l) - (L_{LF}(40,l) - L_{LF}(LBC40))/v_{CF}\,. \\ with\ l &= EBA,\ LBA,\ EBC \end{aligned} \tag{12}$$

The results are displayed in Fig. 15. The circles (triangles) show the resulting partition offsets measured with the laser system, using v_{CF} =22.5 cm/ns (v_{CF} =21.0 cm/ns). The squared markers are the partition offsets, resulting from the analysis [2] of actual beam events, where muons in the LHC beam halo crossed

[1)] This choice is arbitrary

TileCal, travelling parallel to the beam axis. The latter analysis is independent of v_{CF} since it does not rely on the laser system. The best agreement with the beam measurement is achieved with 21.0 cm/ns.

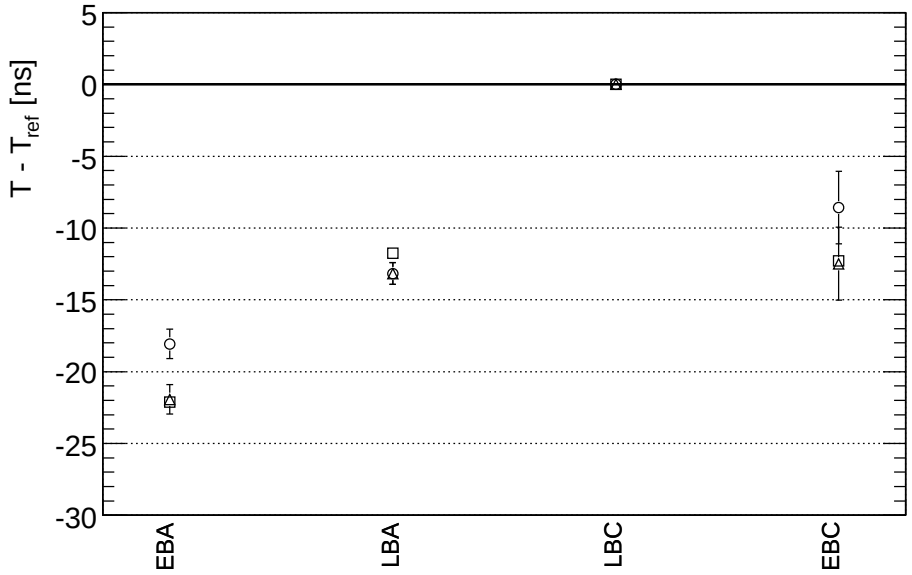

Figure 15: The delays between the different TileCal partitions obtained using laser events inside an ATLAS combined run with v_{CF} =22.5 cm/ns (circles) and v_{CF} =21 cm/ns (triangles). The TileCal drawer LBC40 is used as time reference. The result from the laser is compared to the partition offsets derived in Ref.2 from events triggered by muons from the LHC beam halo (squares).

5 Timing Difference between Gains

In physics mode, the TileCal signals are read out either through a low gain or high gain output depending on the amplitude of the incoming analogue signals. The electronic path along the two chains is not exactly the same, leading to an expected time difference between the high and low gain paths.

To study this effect we analysed a special laser run, where both the low and high gain channels were read out and recorded for analysis, thus allowing one to measure the low gain versus high gain time difference in each channel. For this study the challenge is to choose a laser filter and intensity configuration that allows for large enough signals in the low gain output, without saturating the high gain. After trial and error, filter 2 together with the laser intensity setting of 23,000 were chosen. Despite this effort about 12% of all PMT's had to be removed from the present study due to high gain saturation in some channels or too low amplitude in others. This is a consequence of a non-uniform light intensity distribution to all the drawers, given the current characteristics of the laser distribution system. This can nevertheless be adjusted further, using the screws at the patch panel between the liquid fibers and the laser fibers in the USA15 counting room.

The measured difference, ΔT_{gain}, between the high gain and low-gain paths, for a PMT i is defined in the following way:

$$\Delta T_{gain}(i) = T_{fit}^{HG}(i) - T_{fit}^{LG}(i). \tag{13}$$

The quantity $\Delta T_{gain}(i)$ is histogrammed in Fig. 16 for the 88% of TileCal channels, where the high gain does not saturate, and the low gain signals are of sufficient size. A gaussian fit is performed, leading

to a mean high gain versus low-gain difference of 2.3±0.4 ns. This result is consistent with earlier studies [15] of laser events during testbeam. Reference [15] measures a time difference of 2.2±0.6 ns between the two gains.

The fit method used to measure the time at the maximum of the pulse, relies on the expected pulse shape. To investigate the effect of a possible gain dependence of the pulse shape on the time difference between gains, we rederive the gain difference, using a pulse shape independent method. Following Ref. [15] we adopt the so-called "differential algorithm" to calculate the time of the pulse maximum without relying on a predetermined pulse shape. Hence the T_{fit}'s in Eq. 13 are replaced by $T_{differential}$. The result is shown in Fig. 17. From this histogram the time difference between the low and high gain paths is estimated to 1.9±0.3 ns. The correlation between the result of the fit method and the differential method is shown in Fig. 18. Taking into account the correlation between the two measurements, the significance of the difference between the two method is found to be 1.9. Therefore we conclude that the fit method and the differential algorithm give consistent results, thus confirming a mean time difference between low and high gain of the order of 2 ns. The difference between low and high gain nevertheless varies with a standard deviation of 0.4 ns from channel to channel. Therefore we recommend the high to low gain time difference to be measured for all channels individually.

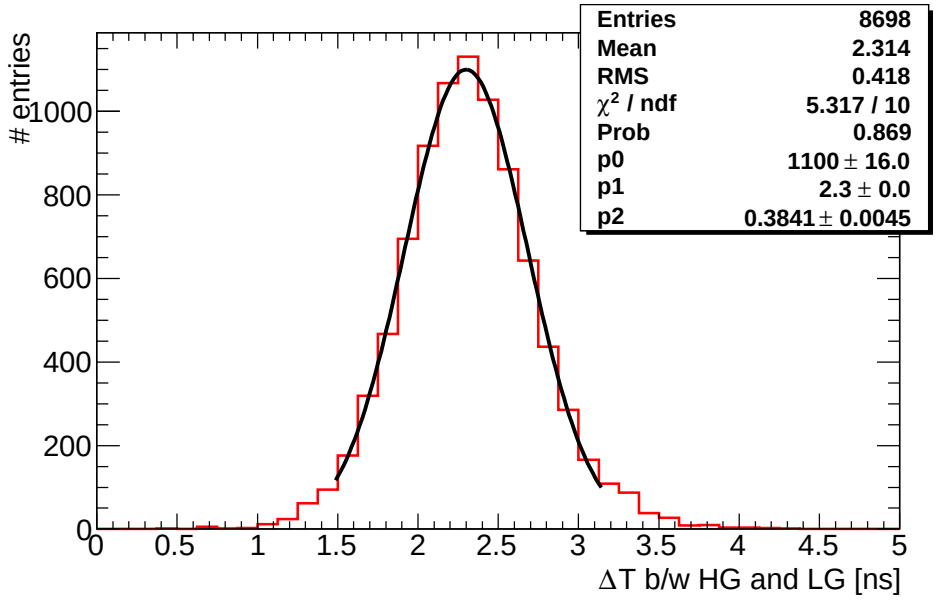

Figure 16: Time difference between high-gain and low-gain using the fit method.

6 Uncertainties

In this section we summarise the various sources of uncertainty on the TileCal timing as derived in this study. It should be noted that the time difference between high gain and low gain needs to be measured for each channel; thus this systematic effect is quantified and does not need to be considered as an uncertainty. If the high gain - low gain difference is not quantified per channel then it would become the leading uncertainty on the TileCal timing. Table 1 summarises the uncertainties detailed in the sections below.

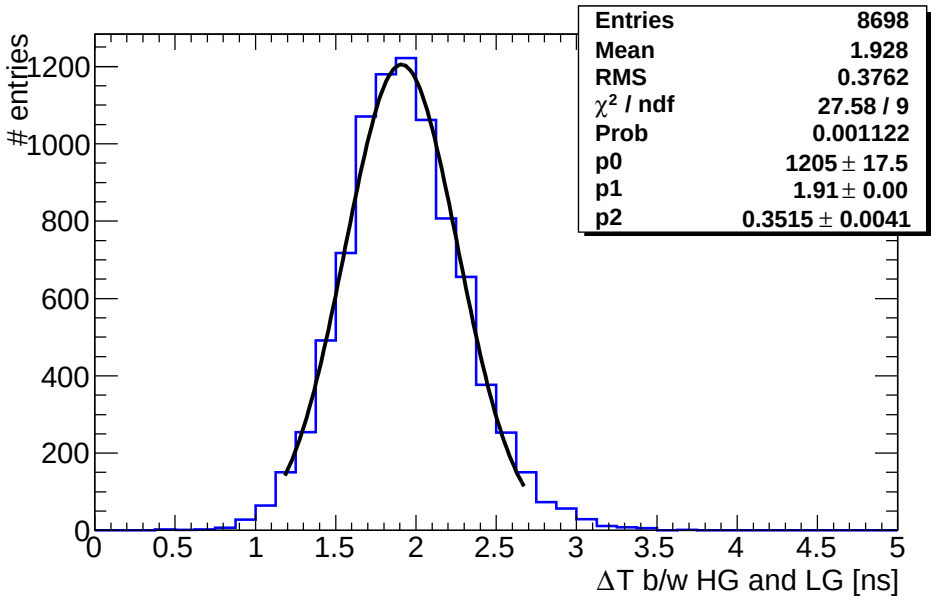

Figure 17: Difference between high-gain and low-gain using the differential algorithm.

6.1 Laser Fiber Lengths

The study of the time difference between even and odd PMT's in barrel drawers (Fig. 8) yields an estimated uncertainty due to laser fiber length of 1.2 ns.

6.2 Pulse Shapes

The fit method relies on the pulse shape of the laser pulses. A systematic comparison of the pulse shapes over the installed TileCal and comparison between physics pulse shapes and laser pulse shapes remains to be carried out. There is a potential bias in the value of T_{fit} if the wrong pulse shape is used to fit the pulse. In Sec. 5 two methods were used to extract the maximum time of the pulse, the standard T_{fit} method as implemented in the TileCal reconstruction for the laser events, and a second method, so-called differential method, which does not rely on pulse shape. We take the difference between the two methods, namely 0.4 ns, though not inconsistent with a statistical fluctuation, as a systematic uncertainty on T_{fit} due to incorrect pulse shape.

6.3 Fit Method Timing Resolution

The fit method has an intrinsic time resolution, which is dependent on the light intensity or equivalently the energy deposited in a TileCal cell. As illustrated in Fig. 12 the distribution of time difference between PMT one and any given PMT is of the order of 0.5 ns for the light intensity used in this analysis. Therefore we infer an approximate per-channel time resolution of $0.5/\sqrt{2} = 0.35$ ns.

6.4 Clear Fiber Routing

As mentioned earlier in Section 3.4, there is an uncertainty in the exact routing of the clear fibers in the second half drawer of TileCal. This is due to the fact that shortly after the start of the TileCal drawer production, the routing scheme was slightly changed, leading to possible differences of 11.6 cm between

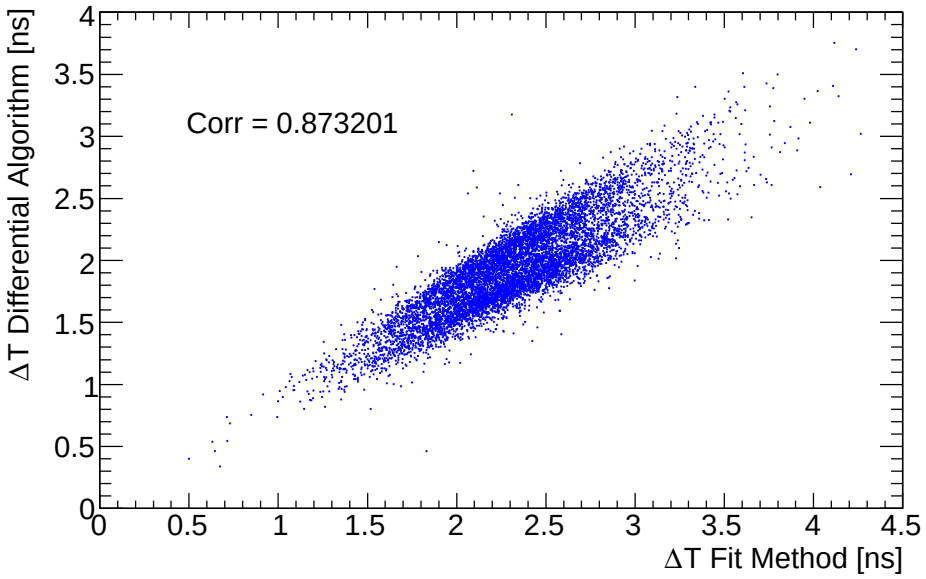

Figure 18: Correlation between the result of the fit method and the differential algorithm.

expected and actual clear fiber lengths [20]. The exact point in time when the change of routing came into effect is not known. This leads to an uncertainty of 11.6 cm in the clear fiber lengths of the second half drawers. This lengths corresponds to abotu 0.5 ns, which we consider a source of uncertainty on the exact TileCal timing.

6.5 Speed of Light in Clear and Laser Fibers

The speed of light in the TileCal laser and clear fibers is known up to a certain precision. Various estimates of this velocity are presented in Sec. 3.4. By varying the speed of light in the interval 20 cm/ns to 22.5 cm/ns, inside the drawer and considering the clear fiber routing (which affects the intra-module timing), we obtain a variation of up to 1 ns between the outermost and the innermost digitizers.

The difference of lengths in laser fibers between the TileCal partitions is much larger than differences in length between the clear fiber inside drawers, especially when comparing TileCal barrel and TileCal extended barrel partitions. If the laser system alone was used to derive the time difference between partitions, the resulting uncertainty would be of the order of 10 ns.

Source of uncertainty	Value
Laser fiber lengths	$\pm$1.2 ns
v_{CF} contribution to intra-module	$\pm$1.0 ns
Pulse shape	$\pm$0.4 ns
Fit method time resolution	$\pm$0.35 ns
Clear fiber routing	$\pm$0.5 ns
v_{CF} contribution to inter-partition	O(10 ns)

Table 1: Significant systematic uncertainties affecting TileCal timing. Note that the time resolution of the fit method is dependent on the light intensity or equivalently the energy deposited. The error quoted for the fit method here corresponds to the typical light intensity used in this analysis.

7 Offline Residuals

We showed how to use the delays measured between the different TileCal channels to derive programmable delays, `dskew2` and pipeline offsets Δp to program the TTCrx chips on the digitizer boards, to equalize the measured pulse times over TileCal. After this online equalisation, one can remeasure the spread in time over TileCal with a new laser run. There is a residual spread among channels due to:

- One TTCrx chip serves 6 channels, therefore the time spread among the channels belonging to the same TTCrx chip cannot be reduced online,
- If the online constants for timing equalisation are not perfect in any way, this will appear in any laser run as a non uniform T_{fit}.

7.1 Derivation of the Offline Residuals

The data from a laser run, taken after implementation of the online programmable delays, can be used to measure the departure of the actual TileCal timing from the perfect TileCal timing. During collisions, the clock is synchronised with the collisions, and the perfect TileCal timing is defined as the set of online constants giving a uniform T_{fit}=0 over all TileCal for all particles travelling with the speed of light and coming from the ATLAS interaction region. In the case of a laser run, the perfect timing is achieved if for a given laser pulse, T_{fit} corrected for laser and clear fiber lengths is constant over all TileCal channels, equal to the T_{fit} in a reference channel.

The offline residuals are additional corrections, which are added offline to the T_{fit}'s in each channel, in such a way that T_{fit} is constant over the entire TileCal, giving the perfect timing for laser runs. If the timing of TileCal is well done, then the offline residuals will be small. For drawers where the online programmable delays could not be computed, the offline residuals will be large. In the current TileCal setup which was also used for ATLAS data taking with the first LHC beam, the offline residuals are known for 99% of the TileCal PMT's and their standard deviation is 0.6 ns. These offline residuals can be used for optimal filtering, up to a global constant equal to the phase in a reference PMT, between the pulse maximum and the clock synchronised to the beam. These offline residuals are remeasured after each modification of the online programmable delays and stored in the TileCal offline database COOL.

7.2 Gain Dependence and Optimal Filtering

It was shown in section 5 that there is a substantial difference between low gain and high gain timing. To ensure optimal energy resolution, especially for high energy showers in the calorimeter, one needs to implement online programmable delays derived for the low gain. Thereafter one can take two laser runs, with intensity settings for low and high gain. Thus we can derive the offline residual corrections in the low and high gain. The optimal filtering can then rely on either the low or high gain residuals to extract the phase between the pulse maximum and the sampling clock, depending on the gain of the incoming data to the RODs.

8 Conclusion

A method to equalise the pulse times measured in all TileCal drawers has been developed and applied to about 99% of the TileCal channels. The residual spread for simultaneous laser pulses is of the order of 0.6 ns in each TileCal partition. The laser system was also used to derive the global offset among TileCal partitions, but suffers from the uncertainty on the laser fiber length. Nevertheless a combination of the laser data and beam data can be used to calibrate the lengths of the laser fibers. Finally the main

sources of uncertainties on the TileCal timing are presented. The biggest effect is potentially the timing difference between low and high gain but this uncertainty can be removed if the online programmable delays are derived for a given gain, optimally the low gain, and the offline residuals are then computed for low and high gain separately. This can be done by adjusting the laser intensity to recommended values. The second leading source of uncertainty is the laser fiber length, which should ultimately be calibrated with beam data and which would allow one to independently measure the TileCal timing using beam or laser events.

9 Acknowledgments

We would like to thank the Clermont-Ferrand group for their support of the laser system, and Christian Bohm, João Carvalho, Monica Dunford, Ana Henriques, Martina Hurwitz, Ilya Korolkov, Jose Maneira, Belen Salvachua, Sasha Solodkov, Vakhtang Tsiskaridze, Ximo Poveda, Irene Vichou, Sebastien Viret and Matteo Volpi for precious help, discussions and advice on the various aspects of the timing of TileCal.

References

[1] J. Castelo *et al.*, Algorithms for the ROD DSP of the ATLAS Hadronic Tile Calorimeter, In proceedings of the 12th Workshop on Electronics for LHC and Future Experiments, Valencia, Spain, 2006. Also available at: http://cdsweb.cern.ch/record/1028147?ln=en.

[2] I. Korolkov, M. Volpi, TileCal timing in events with beam, ATLAS presentation, not published.

[3] ATLAS Collaboration, Tile calorimeter technical design report, CERN-LHCC-96-042, http://cdsweb.cern.ch/record/331062.

[4] ATLAS Collaboration, The ATLAS Experiment at the CERN Large Hadron Collider, JINST 3 (2008) S08003, http://www.iop.org/EJ/toc/1748-0221/3/08.

[5] R. Wigmans, Calorimetry. Energy Measurements in Particle Physics, (Oxford Science Publications, Oxford, 2000), ISBN 0198502966.

[6] R. Leitner, V.V. Shmakova, P. Tas, Time resolution of the ATLAS Tile Calorimeter and its performance for a measurement of heavy stable particles, ATLAS Note, ATL-TILECAL-PUB-2007-002.

[7] ATLAS Collaboration, The ATLAS Level-1 Calorimeter Trigger, JINST 3 (2008) P03001, http://www.iop.org/EJ/jinst/.

[8] K. Anderson et al., Design of the front-end analog electronics for the ATLAS tile calorimeter, Nucl. Instrum. Meth. A 551 (2005) 469.

[9] J. Lesser, Development and Test of the ATLAS Tile Calorimeter Digitizer, ISBN 91-7265-973-4 pp 1-75, Ph.D. thesis, Stockholm University, 2004.

[10] Timing, Trigger and control (TTC) Systems for the LHC, http://ttc.web.cern.ch/TTC/intro.html.

[11] M. Ramstedt, Construction and Testing of the TileCal Digitizer and an Evaluation of the Discovery Potential for R-Hadrons at the ATLAS Detector at the LHC, ISBN 91-7155-180-8 pp 1-66, Ph.D. thesis, Stockholm University, 2005.

[12] S. Berglund et al., The ATLAS Tile Calorimeter Digitizer, in proceedings of the Fifth Workshop on Electronics for LHC Experiments, p79, Snowmass, 1999, and reference therein.

[13] The Calorimeter Data Management Unit (DMU), http://www.sysf.physto.se/ klere/tile-dmu/.

[14] R. Teuscher, Methods of energy reconstruction in TileCal, Talk given at 'TileCal MC+Tools Meeting', June 2003, available at http://indico.cern.ch/conferenceDisplay.py?confId=a031558.

[15] T. Del Prete, I. Vivarelli, Timing of the Tile Calorimeter using laser events, ATL-TILECAL-2003-009.

[16] V. Garde, Controle et etalonnage par lumiere laser et par faisceaux de muons du calorimetre hadronique a tuiles scintillantes d'ATLAS., Ph.D. thesis, Clermont-Ferrand 2. Lab. Phys. Corpusc. Cosmol, http://cdsweb.cern.ch/record/722109/files/CM-P00048399.pdf, 2003.

[17] Ilya Korolkov, Vakhtang Tsiskaridze, et al., Laser fibers OTDR measurements, Talk available at: http://indico.cern.ch/conferenceDisplay.py?confId=30819.

[18] Mitsubishi, Eksa Optical fiber division, Laser fibers manufacturer specifications, Available at:http://www.i-fiberoptics.com/pdf/GH4001.pdf.

[19] ATLAS CVS repository, http://atlas-sw.cern.ch/cgi-bin/viewcvs-atlas.cgi/groups/stockholm/TileCal/LaserTiming/.

[20] Ana Henriques, Private communication.

[21] TileCal barrel clear fiber lengths, http://atlas.web.cern.ch/Atlas/SUB_DETECTORS/TILE/ production/optics/instrumentation/Blengths.htm.

[22] Report from the TileCal Clear Fibers Committee, http://atlas.web.cern.ch/Atlas/SUB_DETECTORS/TILE/ production/optics/instrumentation/relatorio.html.

[23] TileCal extended barrel clear fiber lengths, http://atlas.web.cern.ch/Atlas/SUB_DETECTORS/TILE/ production/optics/instrumentation/EBlengths.htm.

Appendices

A Clear Fibers in Barrel Modules

PMT nbr		Length [cm]	Correction [ns]	Digitizer nr.
1	2	167.1	0	#1
3	4	178.7	0.52	
5	6	190.3	1.03	
7	8	201.9	1.55	#2
9	10	213.5	2.06	
11	12	225.1	2.58	
13	14	236.7	3.09	#3
15	16	248.3	3.61	
17	18	259.9	4.12	
19	20	271.5	4.64	#4
21	22	283.1	5.16	
23	24	294.7	5.67	
25	26	201.9	1.55	#5
27	28	213.5	2.06	
29	30	225.1	2.58	
31	-	236.7	3.09	#6
-	34	248.3	3.61	
35	36	259.9	4.12	
37	38	271.5	4.64	#7
39	40	283.1	5.16	
41	42	294.7	5.67	
43	-	306.3	6.19	#8
45	46	317.9	6.70	
47	48	329.6	7.22	

Table 2: The Barrel clear fiber lengths [21], [22] and the corresponding corrections computed using a light velocity of 22.5 cm/ns.

B Clear Fibers in Extended Barrel Modules

PMT nbr		Length [cm]	Correction [ns]	Digitizer nr.
1	2	51.1	0	#1
3	4	62.7	0.52	
5	6	74.3	1.03	
7	8	85.9	1.55	#2
9	10	97.5	2.06	
11	12	109.1	2.58	
13	14	120.7	3.09	#3
15	16	132.3	3.61	
17	18	143.9	4.12	
21	22	167.1	5.16	#4
23	24	178.7	5.64	
29	30	213.5	7.21	#6
33	34	236.7	8.25	
37	38	259.9	9.28	#7
41	42	283.1	10.31	
43	44	294.7	10.83	

Table 3: The Extended Barrel clear fiber lengths [23], [22] and the corresponding corrections computed using a light velocity of 22.5 cm/ns.